IOP Publishing — Journal of Micromechanics and Microengineering

J. Micromech. Microeng. **21** (2011) 075004 (9pp) doi:10.1088/0960-1317/21/7/075004

MEMS-plunger platform for tunable terahertz wire laser at ∼5 K

Q Qin[1,2] and Q Hu[1,2]

[1] Department of Electrical Engineering and Computer Science, Cambridge, MA 02139, USA
[2] Research Laboratory of Electronics, Massachusetts Institute of Technology, Cambridge, MA 02139, USA

E-mail: qiqin@mit.edu

Received 10 January 2011, in final form 23 April 2011
Published 1 June 2011
Online at stacks.iop.org/JMM/21/075004

Abstract

The tuning of a terahertz quantum cascade wire laser, operated at ∼5 K, is demonstrated using a micro-machined metal or silicon object, called a 'plunger', attached to a MEMS-based two-stage flexure and actuated by a differential micrometer through a piezo-actuator that is de-amplified by a lever system. The heterogeneous system including the plunger, made from a silicon-on-insulator wafer, and a wire laser based on GaAs/AlGaAs material with first-order distributed feedback corrugation, works at liquid helium temperature (∼5 K). The double-stage flexure design enables a frictionless, reversible and continuous tuning over a broad range of ∼330 GHz (∼8.6% of the 3.85 THz center frequency) with single-mode operation.

(Some figures in this article are in colour only in the electronic version)

1. Introduction

Broadly tunable coherent terahertz (THz) sources are highly desired for applications in sensing and spectroscopy [1, 2]. There has been significant interest in using THz quantum cascade lasers (QCLs) for this application [3–5] because of their compact size and relatively high output power. Conventional methods, including external-cavity mirror and grating methods, have been explored with THz QCLs and turned out to be difficult to achieve continuous tuning over a broad range with single-mode operation, mainly due to the poor coupling between the external reflector and the gain medium. The additional requirement of the cryogenic operation of THz QCLs further exacerbated this difficulty. Recently, a substantial improvement of the tuning range in a THz wire laser (figure 1), whose transverse dimension □ is much less than the wavelength (□ $\sim \lambda_o/6$), was demonstrated in our group [6]. This tuning was achieved by manipulating the transverse wave vector with a so-called plunger, which is a moveable side object made up of a small piece of metal or dielectric material, as illustrated in figure 1. The practical implementation of this concept requires controllable and strictly translational movement with a ∼10 nm movement resolution. However, due to a significant stick-slip effect [7] between the plunger and the track at cryogenic temperature, and the lack of a restoring mechanism, the movement of the plunger was discontinuous and irreversible [6], limiting practical applications for this technique. In addition, the tilting of the plunger during its movement significantly reduces the tuning range, which is discussed later. These initially encountered difficulties significantly increase the precision requirement of the alignment and mechanical operation. One possible solution to these problems is using plungers based on micro-electromechanical systems (MEMS).

There is little work reported about the MEMS technology operating at liquid helium temperature. In this work, in a ∼5 K environment, we vary the distance between the plunger and THz wire laser by using a MEMS plunger actuated by a lever-de-amplified differential micrometer through a piezo-actuator, in order to continuously adjust the lasing frequency in a reversible manner. The assembled device of a MEMS plunger and a wire laser is illustrated in figure 2. Because of the small size of both the wire laser die (2 mm × 2 mm) and the MEMS plunger (2.3 mm × 2.3 mm), it is difficult to implement a traditional aligned bonding technique here. In this work, a female–male aligned scheme is used in the assembly between the plunger wafer and the wire laser die, resulting in a better than 10 μm alignment precision. Using a clamp to fix the assembled structure, instead of bonding, avoids the mismatch between the thermal expansion coefficients of the silicon (MEMS plunger) and GaAs (material system for THz QCLs) wafers. A two-stage flexure design is used to isolate

 © 2011 IOP Publishing Ltd Printed in the UK & the USA

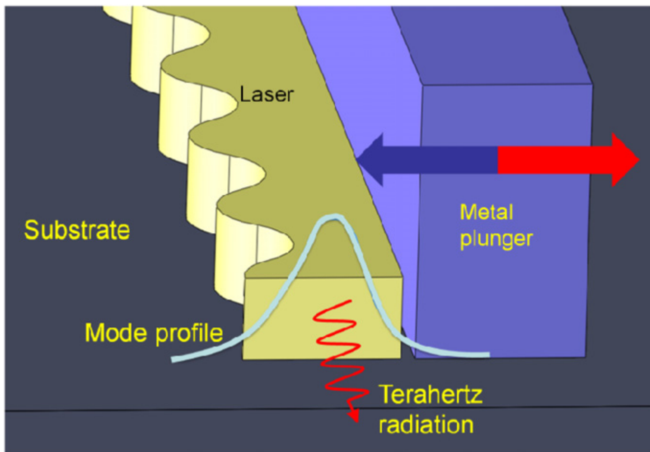

Figure 1. Illustration of the tuning mechanism of the wire laser.

the misalignment from the external actuator. The appeal of the MEMS system is its frictionless, controllable, and reversible movement of the plunger. In addition, the compactness and potential fast tuning speed [6] make this technique very attractive. Our paper reports, for the first time, the integration of MEMS silicon-on-insulator (SOI) technology with THz QCL technology based on the GaAs/AlGaAs material system, which is operated at liquid helium temperature.

2. Basic tuning mechanism

The tuning mechanism is identical to that described in [6], as illustrated in figure 1. The longitudinal wave vector, k_z, of a particular resonant mode in the optical waveguide is fixed by a first-order distributed feedback (DFB) grating, which is formed with the corrugated side wall away from the plunger. The tuning is achieved by changing $k_\perp$, the transverse wave vector. This tuning scheme takes advantage of a trademark feature of wire lasers [8], which is that a substantial fraction of the mode travels outside the solid core of the waveguide in the transverse direction so that it is accessible for manipulation. Pushing a metallic (dielectric) plunger toward a THz wire laser squeezes (expands) the mode in the transverse direction, as demonstrated in figure 3. Consequently, the value of $k_\perp$ increases (decreases) and a resulting blue-shift (red-shift) tuning is achieved, as dictated by the dispersion relation $\omega^2 = \left(k_z^2 + k_\perp^2\right)/\mu\varepsilon$ in a uniform gain medium. Figure 4 plots the projected tuning range when a metal (or dielectric) plunger parallelly approaches a wire laser that has 10.5 μm average width, 3 μm corrugation amplitude, 30 periods and 14.5 μm periodicity. When the plunger moves from 20 μm to 1 μm away from the wire laser, 340 (blue-shift) and 230 GHz (ref-shift) tunings are expected from a metal plunger and a silicon plunger, respectively. This indicates that the displacement range of the plunger should be at least 20 μm to cover the full tuning range. Additionally, the plot illustrates that most of the tuning is from the last few microns' movement of the plunger. This highly nonlinear process requires the plunger to move as close as possible to the wire laser, in order to achieve the largest tuning range. Additionally, a smooth movement of the plunger is crucial for the practical application of this device because of the continuous tunability required by spectroscopy application. Furthermore, it is necessary to keep the plunger parallel to the flat side of the wire laser throughout the tuning range. When the metal (dielectric) plunger is tilted relative to the flat edge of the wire laser, the mode will be pushed (extracted) longitudinally to the end where the plunger is further from (closer to) the wire laser,

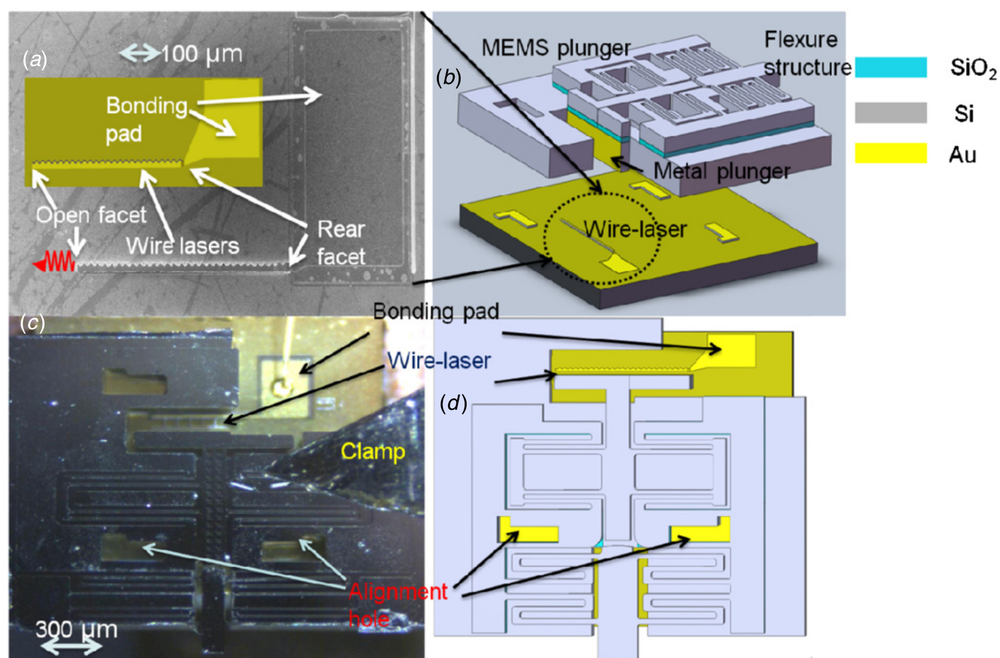

Figure 2. (*a*) Photograph of the wire laser. (*b*) Illustration of the MEMS plunger and the wire laser before assembling. (*c*) Photograph of the top view of the assembled device. (*d*) Illustration of the assembled device corresponding to part (*c*).

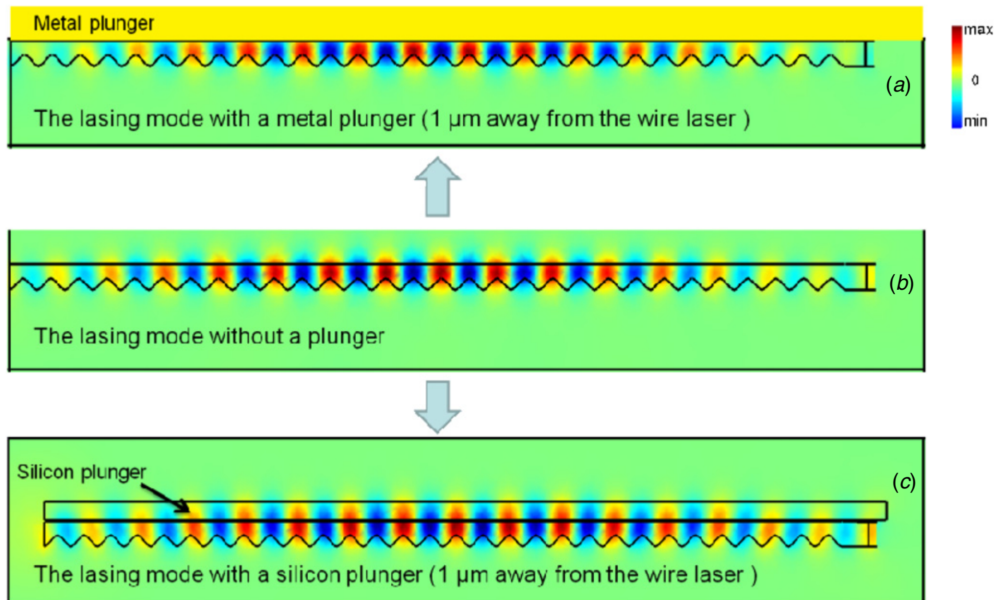

Figure 3. (*a*) Lasing mode with the metal plunger 1 μm away from the wire laser. (*b*) Lasing mode without the plunger. (*c*) Lasing mode with the silicon plunger 1 μm away from the wire laser.

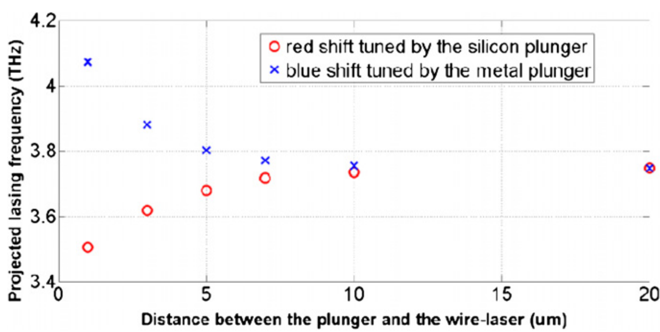

Figure 4. Lasing frequency with metal (blue) and silicon (red) plungers at different positions.

as illustrated in figure 5. Thus the tuning range is reduced dramatically with a metal plunger because the plunger cannot effectively move close to the mode. The simulation shows that even when the tilt angle of the metal plunger is as small as $\sim 0.5°$, the tuning range is reduced to 157 GHz, compared to the 340 GHz without tilting, that is, a reduction by more than a factor of 2. Additionally, the plunger can tilt about the *Y*-axis (figure 6), resulting in an abnormal and undesired tuning behavior [6]. Another important factor underlying the tuning range is the material property of the plunger. This quality will directly affect tuning results because the modal loss will be increased due to the externally introduced material, which is discussed later in the section of tuning results.

3. Design and fabrication

The design of the wire laser and the MEMS plunger must take into account several critical constraints that interleave with each other. Firstly, due to the preciousness of the MBE-grown QCL wafer, the size of the wire laser die should be limited in the range of a few millimeters. This also limits the size of the MEMS plunger because it will reside on the

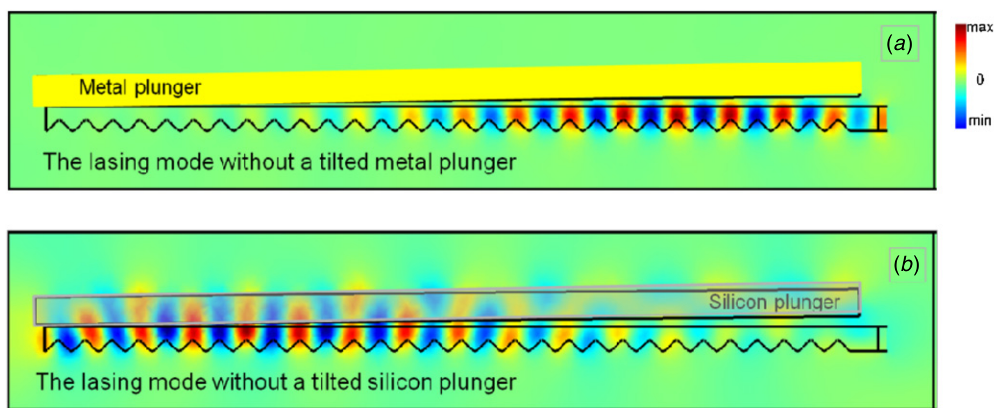

Figure 5. (*a*) Lasing mode with the metal plunger tilted by $\sim 0.5°$. (*b*) Lasing mode with the silicon plunger tilted by $\sim 0.5°$.

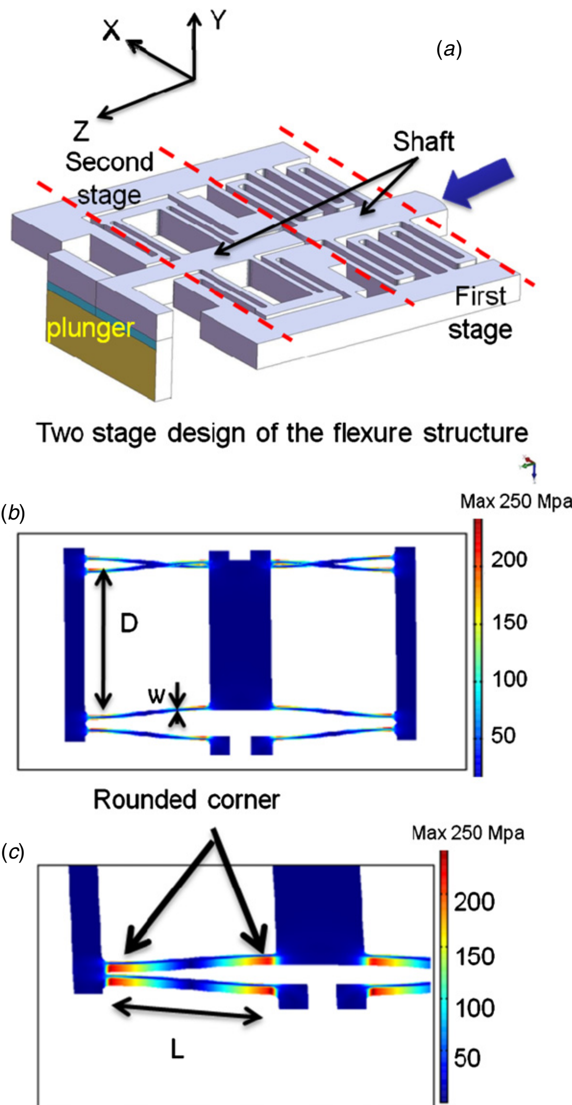

Figure 6. (*a*) Illustration of the flexure structure. (*b*) and (*c*) simulated results of the stress in the flexure structure with ~20 μm displacement.

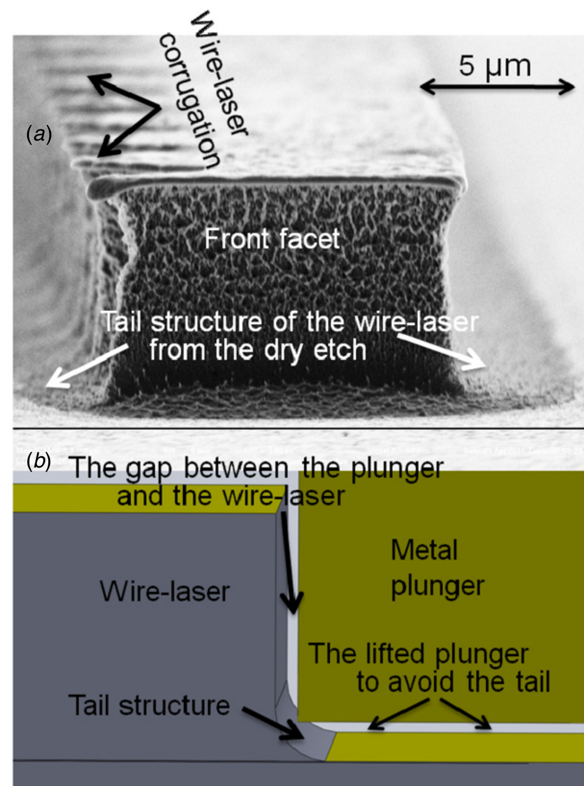

Figure 7. (*a*) SEM picture of the front view of a wire laser to illustrate the tail structure in the bottom corner of the wire laser. (*b*) Schematic of the lifted plunger to avoid the tail structure.

wire laser die. Secondly, to minimize the tilt about the *X*- and *Y*-axes, the spring design of the MEMS should have larger torsional stiffness about the *X*- and *Y*-axes (figure 6). Thirdly, the alignment error should be minimized between the MEMS wafer and the wire laser die. Fourthly, at the liquid helium temperature (~5 K), the maximum displacement of the plunger should be larger than 20 μm to enable a full tuning range, which was discussed earlier. The assembly scheme between the MEMS wafer and wire laser should avoid the possible problems caused by the thermal expansion coefficient mismatch during the cooling process.

Combining all of these considerations, we have come up with a design that is illustrated in figure 2. A complete device is assembled from two components, a wire laser and a MEMS plunger, which were fabricated separately. The wire laser followed the same fabrication steps and used the same MBE-grown wafer as in [6] (wafer VA0094, design FL183S, which is a resonant phonon design). This design has a gain peak of around 3.8 THz. The device has 10.5 μm average width , 3 μm corrugation amplitude, 30 periods and 14.5 μm periodicity. The bonding pad is in the corrugation side of the wire laser to avoid the interference with the plunger movement. Three alignment extrusions on the wire laser die are 10 μm high, which is the same height as the wire laser. These extrusions are used to align the MEMS plunger and the wire laser, which is illustrated in detail later. One important feature of a real wire laser is the tail structure (figure 7), from non-uniform dry etching, in the bottom corner of the flat side wall. Thus, the bottom of the plunger is 1.5 μm higher than the substrate surface of the wire laser die in order not to be blocked when it approaches the wire laser.

The MEMS plunger is fabricated from a SOI wafer. The features are defined in both handle side (on which the plunger is attached) and device layer (which can be pushed by an external actuator) of the wafer (figure 8). The plunger is fabricated in the handle side, which is 500 μm thick to give a rigid mechanical support. The movable flexure structure is implemented in the device layer, whose thickness is chosen as 50 μm to ensure enough stiffness about the *X*-axis (figure 6), which is explained later in detail. The plunger in the handling side is attached with the moveable flexure structure by a 1 μm SiO_2 layer (figures 2(*b*) and 6(*a*)). The movable flexure structure suspends on the handle side after etching the embedded SiO_2 sacrificial layer.

The design was carried out from three aspects to minimize the tilting possibilities about both *X*- and *Y*-axes. First, a

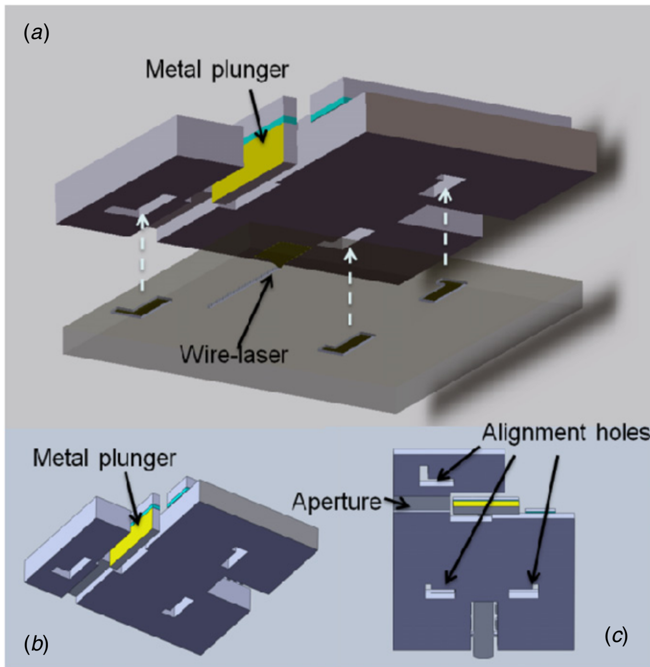

Figure 8. (*a*) Illustration of the alignment scheme between the wire laser and MEMS plunger. (*b*) and (*c*) detail of the backside of the MEMS-plunger wafer from tilted (*b*) and bottom (*c*) view.

two-stage flexure design is used to enable a restorable and non-tilting MEMS plunger, as illustrated in figure 6. The first stage in this design can isolate the second stage, which is attached with the plunger, from the external misalignment of the actuator. The shape of the front of the first stage has a circular-arc edge (figure 11), which avoids transferring the torque about the *Y*-axis to the second stage. Even when the first stage is actuated slantways, because of the front arc shape, the tilting of the second stage is minimized as long as the friction between the first-stage front and the second-stage tail is not too large. The stiffer design of double compound rectilinear spring is used in the second-stage design to minimize the tilt of the plunger at the expense of a smaller movement range compared to that of the first stage, in order to ensure greater precision.

Secondly, since the alignment quality between the MEMS plunger and the wire laser is crucial to the performance of the tunable wire lasers, three L-shape alignment elements (figure 8) are used to minimize the initial tilting about the *Y*-axis. These three L-shape extrusions on the wire laser wafer can click with the three L-shape holes in the MEMS-plunger wafer. The size of the holes is only 10 μm larger than the extrusion structure to optimize the precision. The distance between the three alignment elements is 1200 μm, which has been maximized under the constraints of the die size. In this configuration, the worst case will give a $\sim 0.5^\circ$ ($\sim 180/120\pi$) tilting. In addition, the alignment hole in the MEMS wafer is through the whole SOI wafer to facilitate the alignment when the extrusion can be seen through the holes. During the assembly process, the MEMS wafer is first roughly aligned with the wire laser die under a microscope. Then the MEMS wafer is nudged by a micrometer until the alignment holes click with the extrusions and the laser die is forced to move with the MEMS wafer together. The difficulty of this alignment lies in the 10 μm thickness of the alignment structure. The alignment function of this 10 μm thick structure could be easily disabled by dust, which tends to be larger than 10 μm. Or if the edge of the extrusion or the holes is not sharp, the clicking effect will not function well because it is very easy to slide the MEMS structure ($\sim$500 μm thick) onto the 10 μm high structure. Thus a clean surface and sharp edges of the alignment structure are crucial for a good alignment. Therefore, solvent cleaning and nitrogen gas blowing were performed before the alignment to remove dirt or dust.

Thirdly, the plunger design needs to take into account the possibility of tilting about the *X*-axis (figure 6). The plunger mass and device layer thickness should be designed carefully to ensure no severe tilt of the second stage about the *X*-axis. The torsional stiffness of a simple leaf design about the *X*-axis, which is proportional to the torsional stiffness of a double compound rectangular design, is $Eh^3\square D^2/2L^3$, where L, $\square$, h, W, D and E are the length, width and height of the beam, the distance between the two beams, and Young's modulus, respectively. On one hand, a large height is preferred to increase the torsional stiffness about the *X*-axis. On the other hand, if the height is too large, it can cause dry-etching difficulties due to a large aspect ratio. Therefore, a 50 μm thickness of the device layer is chosen and the size of the plunger is $\sim$700 μm $\times$ 50 μm $\times$ 550 μm. Additionally, as indicated by the torsional stiffness equation, to optimize this value, D should be maximized under the size constraint. Here, D was chosen as 250 μm for the second stage. A mechanical FEM simulation was performed, using a commercial software program COMSOL 3.5, to confirm that the design requirement is satisfied. It showed a negligible tilt about the *X*-axis resulting from the plunger mass.

The possibility of catastrophic failure with the maximum displacement of the plunger should be considered after minimizing the tilting. The yield stress of silicon is 5–7 GPa at room temperature and the data at 5 K are not known. In addition, because any defect from fabrication in the beam can cause failure as the stress is accumulated, the structure strength is not easily predicted before actual implementation. Thus a large safety factor is necessary to ensure non-failure displacement of the flexure. The largest stress in a cantilever beam is $3E\square S/2L^2$ [9], where S is the maximum displacement. As discussed in the introduction, at least 20 μm displacement is required to cover the full tuning range. In the actual design, 40 μm maximum displacement of the second stage was used to yield a large safety margin. The non-actuated gap between the second-stage tail and the front-stage front is $\sim$9 μm. Thus the required displacement range of the first stage is $\sim$9 μm larger than the second stage. Therefore, a softer three-fold spring is used in the compound spring design of the first stage to ensure a larger displacement range. As indicated by the above equation, to achieve the 40 μm displacement range at $\sim$5 K, thin and long beams should be used to avoid material failure. On the other hand, to avoid buckling of the second stage, thick beams should be used to increase the stiffness. This tradeoff between the two underlying factors results in the 20 μm thick and

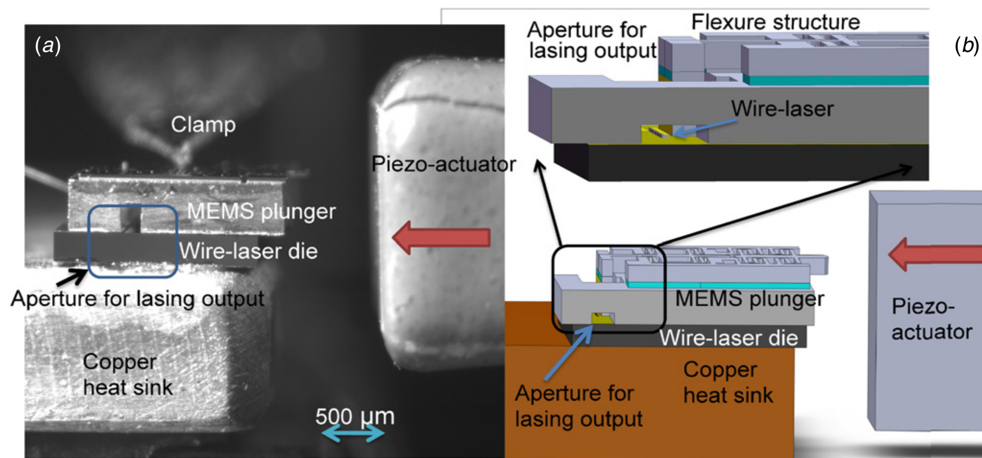

Figure 9. (*a*) Photograph of the side view of an assembled device. (*b*) Illustration of the relative position of the wire laser and the output aperture corresponding to part (*a*). The upper part is the blow-up of the output aperture.

650 μm long beam design in the first stage and 25 μm thick and 700 μm long in the second stage. In addition, all of the corners of the flexure structure were rounded by a 25 μm radius halo (figure 6(*c*)) to avoid the stress concentration in the corner. A FEM simulation was performed to evaluate the maximum stress under the largest displacement. This simulation (figures 6(*b*) and (*c*)) shows that the maximum stress is 250 MPa with ~20 μm displacement. This gives a safety factor of ~20 at room temperature, which should yield a sufficient margin to compensate for the property change of silicon at cryogenic temperature.

Besides the non-tilting and non-failure displacement at liquid helium temperature, several other factors need to be addressed. First, the bottom surface of the plunger is ~1.5 μm elevated from the bottom of the supporting structure, to avoid interference of the tail structure of the wire laser (figure 7). Second, beside the plunger head, as illustrated in figure 9, there is a ~250 μm deep and 200 μm wide trench, which is used as an aperture to out-couple the laser emission. The depth of 250 μm was chosen so that the light can come out and the remaining ~250 μm handle wafer is still strong enough to survive during the later alignment step.

In the current design, because of the limited wafer size, a comb-driver is not integrated with the MEMS chip yet. Instead, compared to the actuation system in [6], between the lever end and the MEMS plunger a piezo-actuator (Thorlab AE0505D08F), which has a maximum displacement of 9.1 μm and a resonance frequency of 138 kHz at room temperature, is added to achieve fine and fast tuning (figure 7(*b*)). This piezo-actuator is chosen because it has the largest displacement among the available ones, given the space limitation of the cryostat. However, at cryogenic temperature, the maximum displacement is estimated to be reduced to ~1–2 μm, which cannot cover the whole tuning range. In an actual operation, sequentially, the lever is pushed by the micrometer to realize coarse tuning and the piezo-actuator can then be used to realize fast fine tuning by pushing the MEMS plunger. In this fine tuning system, the MEMS plunger has a smaller resonance frequency (~15 kHz from FEM simulation), which determines the maximum tuning speed.

The MEMS-plunger fabrication process is outlined in figure 10. The process began with lithography on the handle side and dry etching for a ~1.5 μm depth. Thus, the bottom of the plunger was lifted by 1.5 μm to avoid the interference from the tail structure of the wire laser, which is discussed earlier. Then 3 μm thick SiO_2 was deposited on both sides of the wafer by plasma-enhanced chemical vapor deposition (PECVD), followed by annealing at 1000 °C for ~1 h to increase the oxide strength during the later long dry etching. Both sides of the SiO_2 were patterned by standard lithography and BOE etching, and were used as hard masks. After this, a 10 μm thick photoresist was spun on the handle side of the wafer and patterned in such a way that all of the through holes were open and the output aperture mentioned earlier was covered by photoresist. Then silicon etching was performed for ~250 μm depth by deep reactive ion etching (DRIE) using equipment from surface technology systems. After this etching, the photoresist was stripped by piranha and the handle side of the silicon was etched again until the through holes reached the embedded SiO_2. Thus the different depth etching on one side was achieved by this double mask technique. After the etching on the handle side, two DRIE steps were performed on the device side, even though all of the holes are through all the way to the SiO_2 layer. This two-step process is adapted so that a narrow gap (~9 μm) between the first and second stage can be etched uniformly all the way through. First, only the gap between the first and second stages was exposed to DRIE for ~35 min (~30 μm depth) etching with a thick photoresist mask. Then the photoresist was stripped and the whole device side was etched with annealed SiO_2 as the mask. This DRIE with double mask is necessary to achieve a vertical side wall of the beams of the flexure structure, which is necessary to avoid structure failure [10] when the beams are deflected. It is desirable to have DRIE reach the stop layer (SiO_2 in this case) simultaneously across the whole area because any further etching will drill a notch in the bottom corner, which can result in a weakened mechanical structure [10]. However, the gap size between the two stages is only ~6 μm on the mask (figure 10), which is much smaller than other places and will

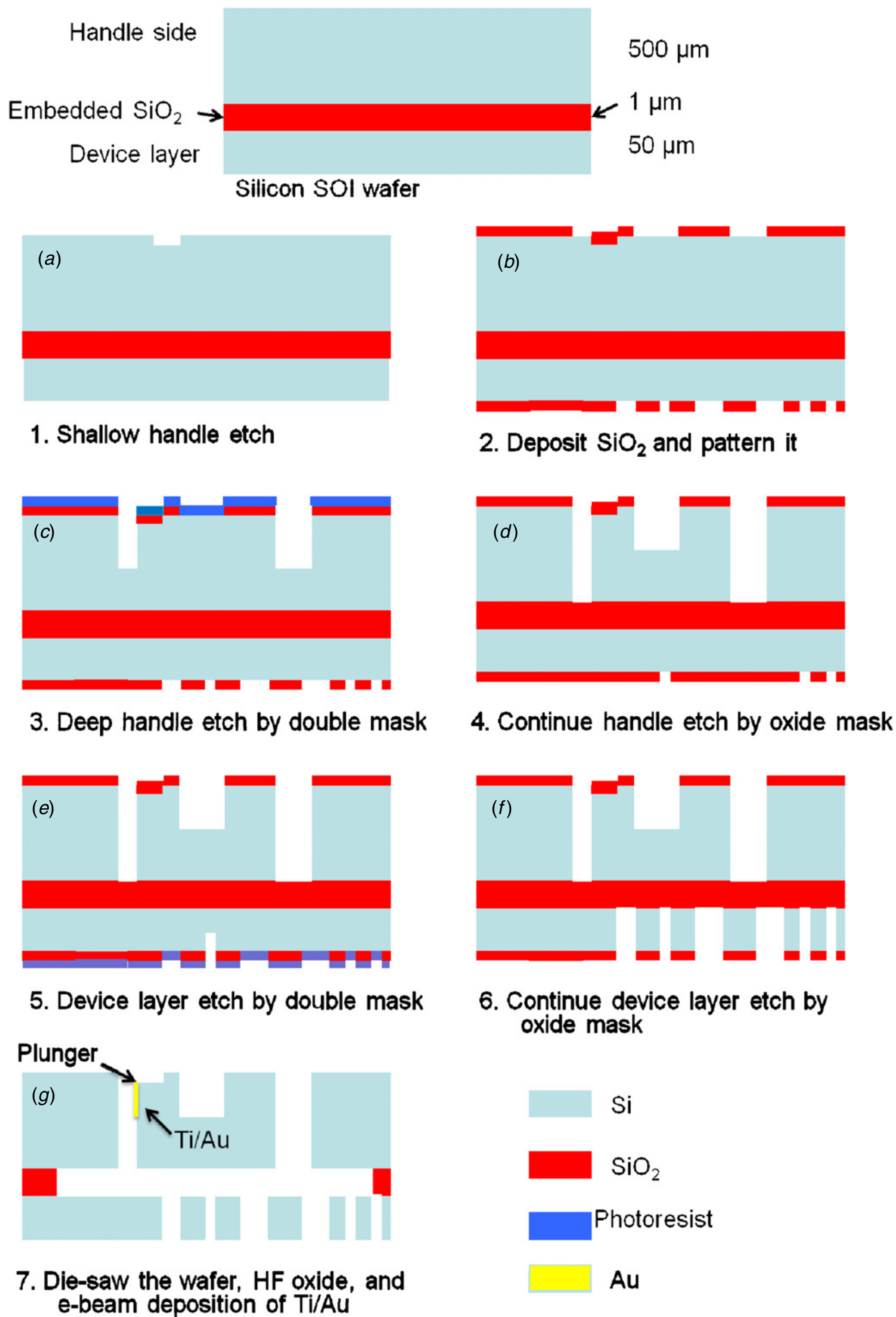

Figure 10. Illustration of the fabrication process.

result in a much slower etching rate. Thus, first only this gap was etched for ~35 min and then it reached the embedded SiO_2 simultaneously with the other area during the second DRIE etching. Then the wafer was divided into a separated MEMS chip by die saw. To release the flexure structure, a diluted (49% HF:water = 1:5) HF etchant was used to etch away embedded SiO_2. Because of a much larger area, the SiO_2 layer under the plunger was only partially removed from the perimeter (~20 μm), leaving the plunger still mechanically attached to the device side that can be pushed by an external actuator. Finally, the side wall of the plunger was coated with Ti:Au by directional e-beam deposition.

4. Measurement and results

After the wire laser and plunger were fabricated separately, they were aligned and assembled according to the pre-defined

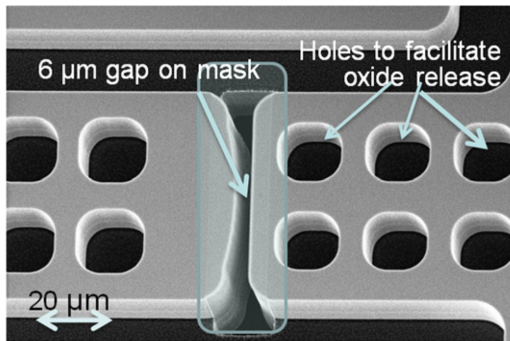

Figure 11. SEM picture of the small gap between the front of the first stage and the tail of the second stage.

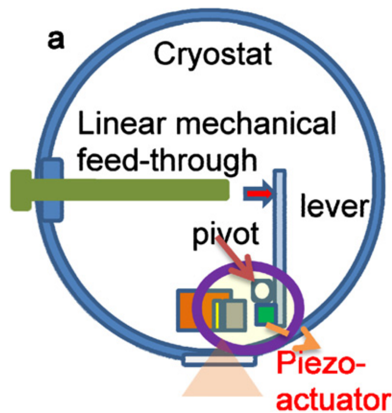

Figure 12. Schematics of the cryostat setup.

alignment holes and extrusions on the plunger and laser wafers. The gap between the plunger and the flat side of the DFB laser is ∼20 μm in a non-actuated position. The external differential micrometer can push the plunger all the way toward the laser. When the micrometer is reversed, the meandering MEMS springs retract the plunger reversibly. The assembled device was mounted in a cryostat (figure 12) for measurement. All spectra were measured at 5 K using a Nicolet 850 spectrometer (purged with N_2 gas) and a Ge:Ga photodetector in the pulse mode with 90 kHz frequency and 200 ns duration.

At ∼5 K, the MEMS plunger functioned as expected without structural failure. A continuous tuning of 330 GHz, or 8.6% fractional tuning, was achieved with MEMS plungers and a device with 10.5 μm average width, 3 μm sinusoidal grating modulation, 30 periods, and a grating period of $\Lambda =$ 14.5 μm. A Si plunger enables ∼30 GHz tuning, compared with ∼300 GHz achieved using a metal plunger. The range of blue-shift tuning (with the metal plunger) is impressive and slightly less than the predicted tuning range (340 GHz), possibly due to a small misalignment. However, the tuning range of the red-shift (with the Si plunger) is underwhelming, even compared to that achieved (∼57 GHz) by a rudimentary system that demonstrated an ∼1:2 red:blue tuning range [6]. This is due mostly to the use of a doped Si plunger. When the Si plunger was close to the wire laser, the mode was extracted out of the gain media into the silicon plunger. The mode effectively saw less gain media and this resulted in an increased threshold current. Additionally, the lasing frequency (∼4 THz) coincides with the absorption spectra of the impurities, which causes a significant lasing modal loss when the Si plunger was close to the wire laser. The much larger tuning range from the metal plunger (compared to ∼80 GHz in [6]) was achieved mostly because the MEMS plunger enables controllable and reversible tuning with a more precise alignment, enabling full exploration of the available tuning range. Furthermore, it is obtained from a slightly narrower laser ridge (10.5 μm as opposed to 12.5 μm in the previous work [6]), which has a larger fraction of the mode propagating outside of the waveguide that is accessible for manipulation. The threshold current density, which is an important indicator of the laser performance, increased when the lasing frequency was tuned away from the original frequency without a plunger. This is due both to additional loss introduced by the plungers and more likely to a decreased gain when the frequency is further away from the gain peak. The detailed results and analysis of the electromagnetic performance of the tunable THz wire laser have been reported elsewhere [11].

5. Conclusion

The operation of MEMS-based systems at liquid helium temperature is a great challenge. The successful operation of this tunable THz wire laser presented some demanding requirements, including precise alignment between two different material systems and strict translational movement of the plunger without tilt. The mismatch of the thermal expansion coefficient in the two material systems causes additional complexity. These requirements have been met and the record tuning range of the THz wire laser operated at ∼5 K temperature has been demonstrated.

A frictionless and reversible tuning of 330 GHz has been achieved in this design. This is the first demonstration where silicon MEMS technology has been applied to the tuning of THz QCLs, which is a novel achievement in the combination of the two technologies. The device size is of the order of millimeters, which is very compact compared to other existing THz tuning methods. Furthermore, the implementation of MEMS technology enables fast electrical tuning, which is highly desirable in many spectroscopy applications. In future development, actuators using comb-drives [12] can be integrated with the flexure design, enabling an all MEMS-based tunable THz wire laser whose frequency can be ‘dialed’ electronically.

Acknowledgments

We would like to thank Professor Martin L Culpepper, Professor Jeffrey H Lang and Dr Hanqing Li at MIT for discussions about the MEMS design. This work is supported by NASA and NSF.

References

[1] Mittleman D 2003 *Sensing with Terahertz Radiation* (Berlin: Springer)

[2] Siegel P H 2004 Terahertz technology in biology and medicine *IEEE Trans. Microw. Theory* **52** 2438–47

[3] Lee A W M, Williams B S, Kumar S, Hu Q and Reno J L 2010 Tunable terahertz quantum cascade lasers with external gratings *Opt. Lett.* **35** 910–2

[4] Xu J *et al* 2007 Tunable terahertz quantum cascade lasers with an external cavity *Appl. Phys. Lett.* **91** 121104

[5] Mahler L, Tredicucci A, Beltram F, Beere H E and Ritchie D A 2010 Tuning a distributed feedback laser with a coupled microcavity *Opt. Express* **18** 19185–91

[6] Qin Q, Williams B S, Kumar S, Reno J L and Hu Q 2009 Tuning a terahertz wire laser *Nat. Photon.* **3** 732–7

[7] Baumberger T, Heslot F and Perrin B 1994 Crossover from creep to inertial motion in friction dynamics *Nature* **367** 544–6

[8] Orlova E E 2006 Antenna model for wire lasers *Phys. Rev. Lett.* **96** 173904

[9] Smith S T 2000 *Flexures: Elements of Elastic Mechanisms* (Amsterdam: Gordon and Breach)

[10] Liu A-Q 2009 *Photonic MEMS Devices: Design, Fabrication and Control* (Boca Raton, FL: CRC Press)

[11] Qin Q, Reno J and Hu Q 2011 MEMS-based tunable terahertz wire-laser over 330 GHz *Opt. Lett.* **36** 692

[12] Prest M J, Wang Y, Huang F and Lancaster M J 2008 Silicon comb-drive actuators for low-temperature tuning of superconducting microwave circuits *J. Micromech. Microeng.* **18** 1250003